Slight ligand modifications within multitopic linear hydroxamates promotes connectivity differences in Cu(II) 1-D Coordination Polymers

Mohammed B. Fugu,[b] Joe Coley,[a] Isabella F. Dickinson,[b] James B. Orton,[c] Wim Klooster[c] M. Paul Gleeson[d] and Leigh F. Jones.*[a,b]

[a] *School of Physical, Biological and Forensic Sciences, University of Wolverhampton. Wulfruna Street, Wolverhampton, England, UK, WV1 1LY. Tel: +44(0)1902-32-1180. Email: Leigh.Jones@wlv.ac.uk.*

[b] *School of Natural Sciences, Bangor University, Bangor, Wales, UK, LL57 2DG.*

[c] *UK National Crystallographic Service, Chemistry, Faculty of Natural and Environmental Sciences, University of Southampton, England, UK, SO17 1BJ.*

[d] *Department of Biomedical Engineering, King Mongkut`s Institute of Technology Ladkrabang, Bangkok 10520, Thailand.*

Synthesis of 4-(amino)phenylhydroxamic acid (PC1)

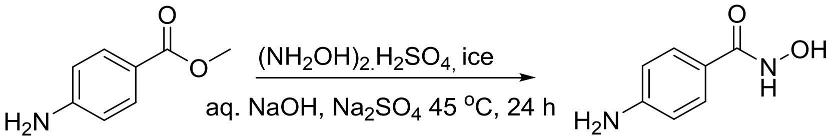

Precursor 1 (PC1)

Hydroxylamine sulphate (6.10 g, 37.00 mmol) and 30.03 g of ice were added to an aqueous solution of NaOH (7.41 g, 185 mmol, 30 cm^3). Na_2SO_4 (0.58 g, 4.44 mmol) and methyl-4-aminobenzoate (5.70 g, 37.00 mmol) were then added to the solution. The mixture was subsequently stirred at 45°C for 24 hrs. The resultant solution was allowed to cool, and the pH was adjusted to 6 using H_2SO_4. When the pH reached 6, a beige coloured solid precipitated out of the solution. The solid was then collected via filtration and recrystallized from hot water and cooled with ice to give PC1 in 60% yield (3.39 g). Elemental analysis (%) calculated as PC1 ($C_7H_8N_2O_2$): C 55.26, H 5.30, N 18.42. Found: C 55.24, H 5.53, N 18.10. ^{1}H NMR (400 MHz d$_6$-DMSO): δ 2.5 (($(CD_3)_2SO$ residual solvent peak), 3.40 (s, H_2O), 5.59 (s, 2H, NH_2), 6.52 (d, J =8.5 Hz, 2H, Ar-H), 7.47 (d, J = 8.6 Hz, 2H, Ar-H), 8.64 (s, 1H, NH), 10.73 (s, 1H, OH). ^{13}C NMR (400 MHz, DMSO): δ (ppm) = 165.5 (CO), 152.0 (C, Ar), 128.7 (2 × CH, Ar), 119.6 (C, Ar), 113.1 (2 × CH, Ar). MS-EI: mz (% Rel. Ab.): 152 (8, {M$^+$}), 134 (8, {M-OH}$^+$), 120 (100, {M-NHOH}$^+$). FT-IR (cm^{-1}): 3410 (s, sh), 3332 (m), 3274 (br), 3025(m), 2789(m), 1645(s, sh), 1589 (s, sh), 1556 (s, sh), 1535 (s, sh), 1502 (s, sh), 1405 (s, sh), 1321 (sh, s), 1292 (sh, s), 1188 (sh, s), 1157 (sh, s), 1094 (sh, s), 1023 (sh, s), 895 (sh, s), 832 (sh, s), 746 (sh, s), 694 (sh, s), 638 (m, sh), 567 (s), 520 (sh), 469 (s, sh), 422 (sh).

Synthesis of (E)-N-hydroxy-4-((2-hydroxy-3-methoxybenzylidene)amino)benzamide (PC2)

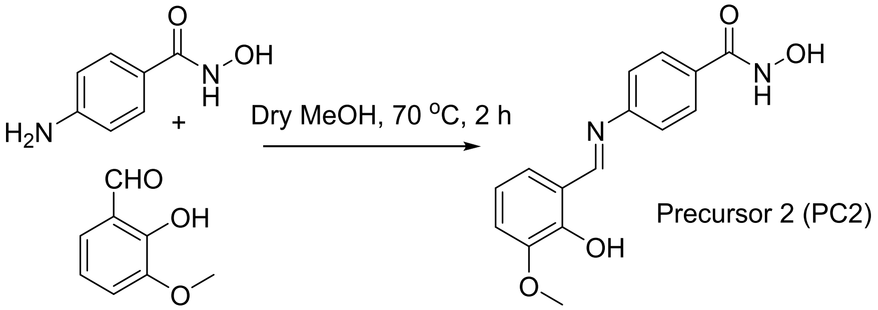

Equimolar amounts of 4-(amino)phenylhydroxamic acid (0.50 g, 3.20 mmol) and *ortho* vanillin (0.50 g, 3.20 mmol) were dissolved in dry methanol (30 cm^3) and the solution refluxed at 70 °C for 2 hours to give a red solid. The solution was then left to cool and subsequently filtered and air dried to give a yield of 55% (0.51 g). ^1H NMR (400 MHz d_6-DMSO): δ 2.51 ($(CD_3)_2SO$ residual solvent peak), 3.83 (s, 3H, OCH_3), 6.53 (d, $J = 8.4$ Hz, 1H), 6.93 (t, $J = 7.9$ Hz,1H, Ar-H), 7.16 (d, $J = 8.0$ Hz, 1H, Ar-H), 7.26 (t, $J = 9.9$ Hz, 1H, Ar-H), 7.48 (d, $J = 8.4$ Hz, 2H, Ar-H), 7.86 (d, $J = 8.3$ Hz, 2H, Ar-H), 8.99 (s, 1H, CH=N), 9.07 (s, 1H, NH), 11.28 (s, 1H, OH), 12.95 (s, 1H, OH). ^{13}C NMR (400 MHz, DMSO-d_6): δ (ppm): 165.0 (CO), 151.0 (C, Ar), 150.8.3 (C, Ar), 148.4 (C, Ar), 131.3 (C, Ar), 128.7 (2 × CH, Ar), 124.4 (CH, Ar), 121.8 (2 × CH, Ar), 119.7 (C, Ar), 119.2 (CH, Ar), 116.3 (CH, Ar), 113.1 (CH, Ar), 56. (CH_3, OMe). MS-EI: m/z (% Rel. Ab.): 286.07 (44; M^+), 254.15 (100; $\{M\text{-NHOH}\}^+$), 224.29 (25, $\{M\text{–C=O-NHOH}\}^+$), 136.22 (20, {M^+ = phenylhydroxamic acid; $[M–C_8H_8NO_2]^+$}). FT-IR (cm^{-1}): 3326 (s), 3066 (w), 2957 (w), 2931 (w), 2899 (w), 2832 (w), 1623 (s), 1595 (s), 1570 (s), 1533 (m), 1513 (m), 1474 (s, sh), 1387 (s, sh), 1367 (w), 1332 (s), 1257 (s, sh), 1202 (s), 1173 (m), 1148 (s), 1111 (s), 1020 (w), 1009 (s), 976 (s, sh), 906 (s), 869 (s), 849 (s), 834 (s), 771 (s, sh), 745 (s), 708 (s, sh), 578 (m), 525 (s), 488 (s), 448 (s), 409 (s).

Synthesis of 4-((2-hydroxy-3-methoxybenzyl)amino)-N-hydroxybenzamide (L_3H_3)

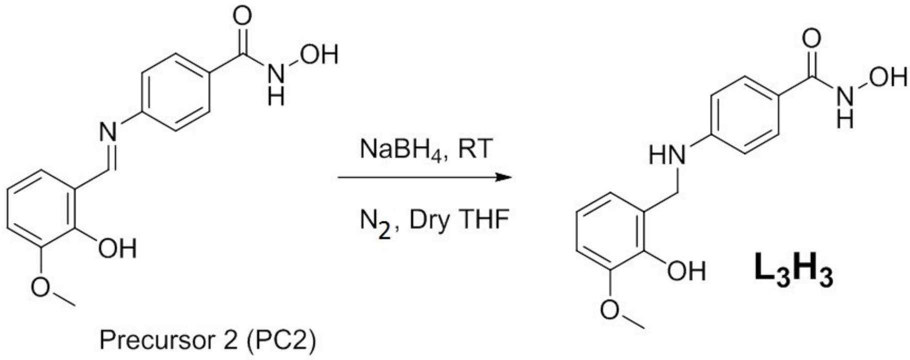

(E)-4-((2-hydroxy-3-methoxybenzylidene)amino)-N-hydroxybenzamide (PC2, 2.00 g, 6.98 mmol) and sodium borohydride (0.40 g, 10.48 mmol) were dissolved in 40 cm^3 dry tetrahydrofuran (THF), and the resultant red solution was stirred under nitrogen conditions at room temperature for 4 hrs. The reaction was then quenched with saturated sodium bicarbonate solution and the organic layer was subsequently extracted with ethyl acetate (3 x 30 cm^3) before washing repeatedly with brine water until all traces of sodium borohydride were removed. The organic layer was then dried with anhydrous magnesium sulphate and the solvent evaporated to dryness to give L_3H_3 in 44% yield (0.88 g). Elemental analysis (%) calculated as $L_3H_3{\cdot}0.7H_2O$ ($C_{15}H_{17.4}N_2O_{4.7}$): C 59.87, H 5.83, N 9.31. Found: C 59.95, H 5.71, N 8.89. ^{1}H NMR (400 MHz d_6-DMSO): δ 2.51 ($(CD_3)_2SO$ residual solvent peak), 3.83 (s, 3H, OCH_3), 4.25 (s, 2H, CH_2), 6.54 (d, 2H, Ar-H), 6.62 (d, 1H, Ar-H), 6.68 (s, 1H, NH), 6.70 (t, 1H, Ar-H), 6.80 (d, 1H, Ar-H), 6.84 (d, 1H, Ar-H), 7.49 (d, 2H, Ar-H), 8.75 (s, 1H, NH), 10.75 (s, 1H, OH), 11.20 (s, 1H, OH). ^{13}C NMR (400 MHz, DMSO-d_6): δ (ppm) = 161.3 (CO), 151.6 (C, Ar), 147.7 (C, Ar), 144.3 (C, Ar), 128.6 (CH, Ar), 127.7 (CH, Ar), 126.1 (C, Ar), 120.6 (CH, Ar), 119.5 (C, Ar), 119.1 (CH, Ar), 112.1 (CH, Ar), 111.4 (CH, Ar), 110.7 (CH, Ar), 56.2 (CH_3, OMe), 40.6 (CH_2). MS-EI: m/z (% Rel. Ab.): 288.11 (5; $\{M^+\}$), 270.30 (5; $\{M\text{-}OH\}^+$), 256.41 (36; $\{M–H_2NO\}^+$), 134.28 (35; {4-aminobenzamide $[M–C_8H_{10}O_2]^+$}), 120.28 (100, {benzamide $[M–C_8H_{10}NO_2]^+$}). FT-IR (cm^{-1}): 3400 (s), 3311 (m), 3209 (m), 2870 (m), 2815 (m), 1608 (s, sh), 1573 (m), 1538 (s), 1502 (s), 1476 (s, sh), 1457 (m), 1434 (m), 1411 (m), 1360 (s), 1335 (s), 1317 (s), 1275 (w), 1262 (s), 1231 (w), 1193 (s), 1181 (w), 1152 (s), 1134 (w), 1081 (s), 1043 (m), 1023 (w), 1005 (w), 987 (w), 894 (s, sh), 877 (w), 823 (s, sh), 759 (s), 727 (m), 717 (m), 617 (w), 568 (w), 529 (w), 511 (s), 535 (s).

Synthesis of (E)-N-hydroxy-4-((2-hydroxybenzylidene)amino)benzamide (PC3)

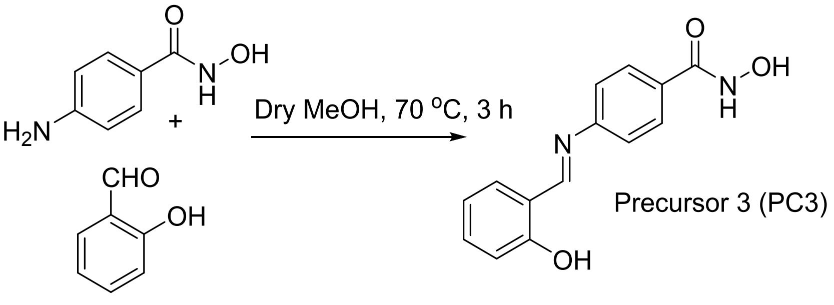

4-(amino)phenylhydroxamic acid (1.00 g, 6.57 mmol) and salicylaldehyde (0.80 g, 6.57 mmol) were dissolved in dry methanol (30 cm^3) and refluxed at 70 ˚C for 3 hours to give PC3 as a yellow solid. The solution was then left to cool and the solid was filtered and air dried to give PC3 in 33% yield (0.56 g). ^{1}H NMR (400 MHz d_6-DMSO): δ 2.51 ($(CD_3)_2SO$ residual solvent peak), 7.00 (t, 2H, Ar-H), 7.44 (d, 1H, Ar-H), 7.49 (d, 2H, Ar-H), 7.70 (d, 1H, Ar-H), 7.88 (d, 2H, Ar-H), 8.99 (s, 1H, CH=N), 9.08 (s, 1H, NH), 11.28 (s, 1H, OH), 12.85 (s, 1H, OH). ^{13}C NMR (400 MHz, DMSO-d_6): δ (ppm) = 164.9 (C, Ar), 164.1 (CO), 160.7 (C, Ar), 151.0 (C, Ar), 134.2 (CH, Ar), 130.1 (CH, Ar), 131.3 (C, Ar), 128.7 (2CH, Ar), 121.8 (2CH, Ar), 119.7 (C, Ar), 119.7 (CH, Ar), 117.1 (CH, Ar). MS-EI: m/z (% Rel. Ab.): 256.08 (20; $\{M\}^+$), 240.23 (24; $\{M\text{-}OH\}^+$), 224.32 (100, $\{M\ –NHOH\}^+$), 196.43 (16, $\{M–C{=}O\text{-}NHOH\}^+$). FT-IR ($cm^{-1}$): 3275 (s), 3026 (br), 2699 (br), 1644 (m), 1617 (w), 1598 (s), 1559 (s, sh), 1489 (s, sh), 1455 (m), 1437 (w), 1409 (m), 1363 (m), 1330 (m), 1309 (w), 1283 (s, sh), 1190 (s), 1181 (w), 1157 (s), 1033 (s), 1011 (s), 982 (s), 910 (w), 899 (s), 848 (s, sh), 779 (m), 750 (s, sh), 740 (w), 698 (m), 683 (m), 541 (w), 525 (s), 481 (s), 442 (s).

Synthesis of N-hydroxy-4-((2-hydroxybenzyl)amino)benzamide (L_4H_3)

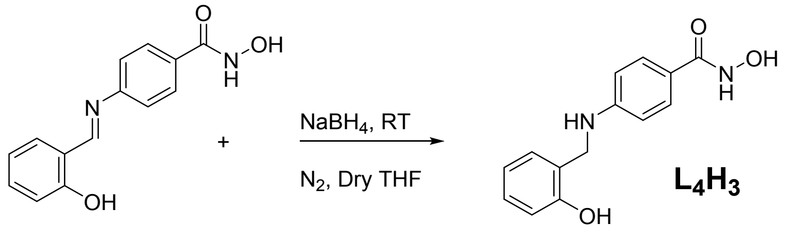

Precursor 3 (PC3)

(E)-N-hydroxy-4-((2-hydroxybenzylidene)amino)benzamide (PC3, 2.00 g, 7.80 mmol) and sodium borohydride (0.44 g, 11.72 mmol) were dissolved in 40 cm^3 dry tetrahydrofuran (THF), and the resultant red solution was stirred under nitrogen conditions at room temperature for 4 hrs. The reaction was then quenched with saturated sodium bicarbonate solution and the organic layer was subsequently extracted with ethyl acetate (3 x 30 cm^3) before washing repeatedly with brine water until all traces of sodium borohydride were removed. The organic layer was then dried with anhydrous magnesium sulphate and the solvent evaporated to dryness to give L_4H_3 in 19% yield (0.36 g). Elemental analysis (%) calculated as L_4H_3 ($C_{14}H_{14}N_2O_3$): C 65.11, H 5.46, N 10.85. Found: C 65.67, H 5.57, N 10.58. ^{1}H NMR (400 MHz d$_6$-DMSO): δ 2.51 ($(CD_3)_2SO$ residual solvent peak), 4.23 (s, 2H, CH$_2$), 6.54 (d, 2H, Ar-H), 6.59 (s, 1H, NH), 6.73 (t, 1H, Ar-H), 6.82 (d, 1H, Ar-H), 7.05 (t, 1H, Ar-H), 7.15 (d, 1H, Ar-H), 7.50 (d, 1H, Ar-H), 8.68 (s, 1H, NH), 9.57 (s, 1H, OH), 10.75 (s, 1H, OH). ^{13}C NMR (400 MHz, DMSO-d$_6$): δ (ppm) = 155.5 (CO), 151.7 (C, Ar), 128.6 (C, Ar), 128.6 (2CH, Ar), 128.1 (C, Ar), 125.6 (C, Ar), 119.6 (CH, Ar), 119.2 (CH, Ar), 119.1 (CH, Ar), 115.3 (CH, Ar), 111.4 (2CH, Ar), 41.3 (CH$_2$). MS-EI: m/z (% Rel. Ab.): 240.26 (10; {M-OH}$^+$), 224.13 (10, {M–NHOH}$^+$), 198.25 (4; {M-C=O-NHOH}$^+$), 134.13 (100, {4-aminobenzamide [M–$C_8H_{10}O_2$]$^+$}), 120.14 (92, {benzamide [M–$C_8H_{10}NO_2$]$^+$}). FT-IR (cm^{-1}): 3194 (br), 2974 (m), 2872 (m), 1604 (s, sh), 1537 (m), 1509 (s), 1454 (s), 1416 (w), 1384 (s), 1334 (s), 1275 (m), 1232 (m), 1183 (w), 1152 (m), 1124 (s), 1079 (s), 1045 (m) 987 (w), 886 (s), 828 (s), 751 (s, sh), 682 (w), 617 (w), 511 (s), 438 (m).

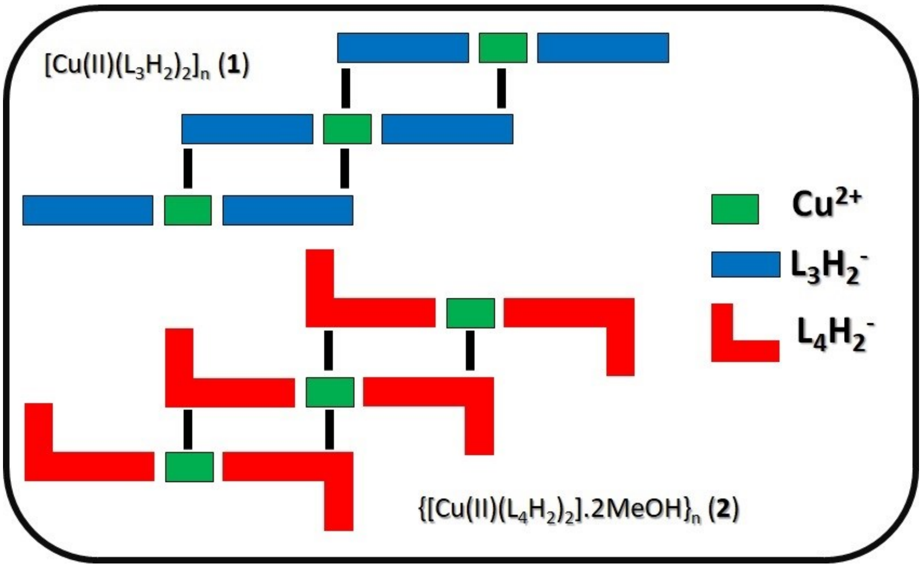

Figure S1 A simplified schematic illustrating the connectivity differences in $[Cu(II)(L_3H_2)_2]_n$ (**1**) and $\{[Cu(II)(L_4H_2)_2].2MeOH\}_n$ (**2**).

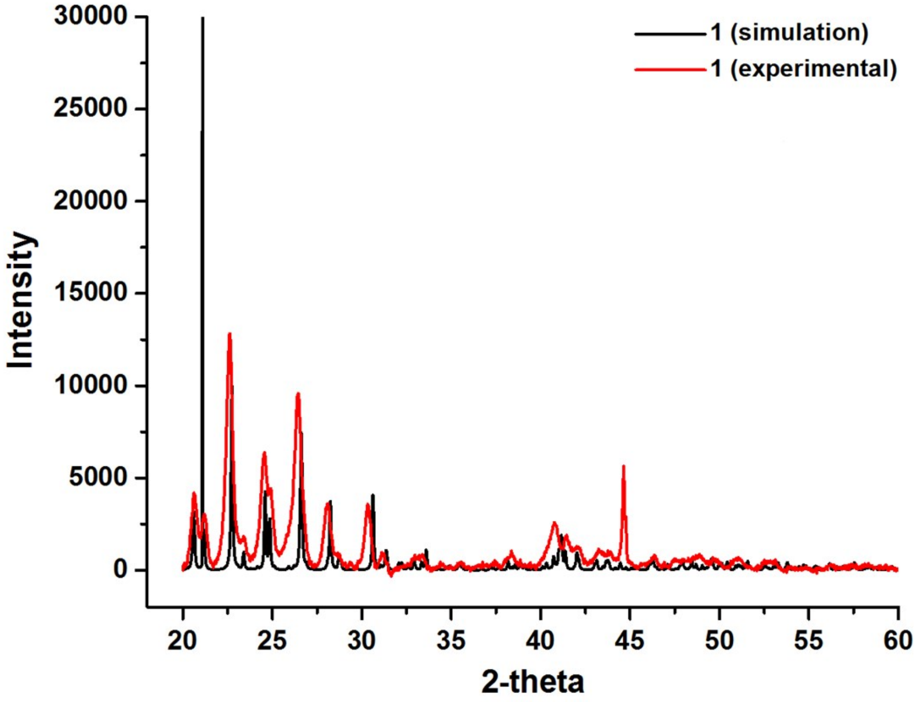

Figure S2 Powdered XRD pattern obtained from a crystalline sample of $[Cu(II)(L_3H_2)_2]_n$ (**1**) (red line) along with its simulated diffraction pattern (black line) produced using single crystal data via the Mercury software package (λ = 1.54056; FWMH (2θ) = 0.1).[1]

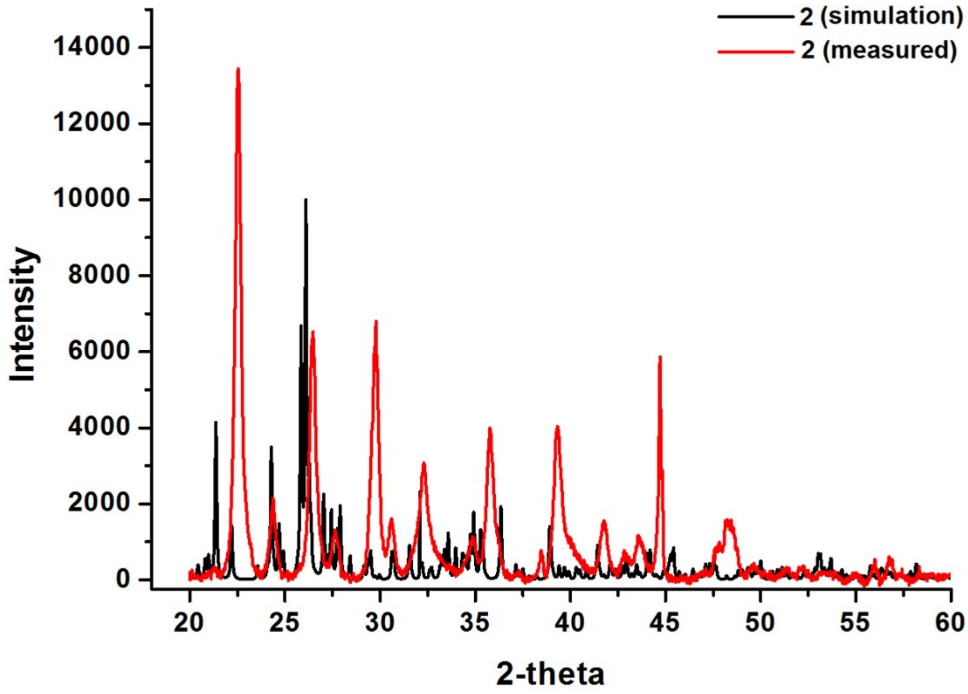

Figure S3 Powdered XRD pattern obtained from a crystalline sample of $\{[Cu(II)(L_4H_2)_2].2MeOH\}_n$ (**2**) (red line) along with its simulated diffraction pattern (black line) produced using single crystal data via the Mercury software package (λ = 1.54056; FWMH (2θ) = 0.1).[1]

Table S1 Magnetic moment data obtained from polycrystalline samples of **1** and **2**.

Sample	$[Cu(II)(L_3H_2)_2]_n$ (**1**)	$\{[Cu(II)(L_4H_2)_2].2MeOH\}_n$ (**2**)
C (calibration constant)‡	1.18	1.18
T (K)	296	296
L (sample length; cm)	2.9	2.0
MW (g mol^{-1})	638.12	642.15
M_0 (g)	0.6511	0.6785
M_1 (g)	0.8144	0.8725
M (M_1-M_0) (g)	0.1633	0.1940
R_0	-0.26	-0.26
R	90	145
R-R_0	90.26	145.26
μ_{eff}	1.69	1.64

‡ Johnson Mathey balance was calibrated using $Hg[Co(II)(NCS)_4]$ prior to use. Magnetic moments calculated using the equations below.

$$\chi_g = c.L.(R-R_o)/10^9.m$$
$$\chi_m = \chi_g.Mw$$
$$\mu = 2.828(\chi_m.T)^{1/2}$$

Table S2 Percentage contribution of elements to the internal and external surface of $[Cu(II)(L_3H_2)_2]_n$ (**1**) using Hirschfeld surface analysis (d_{norm}). *Note:* d_i = internal distance (from the nucleus to the surface), d_e = external distance (between surface and nucleus of nearest neighbour) in Å.

d_i	**d_e**					**d_i total (%)**
	Cu	**O**	**N**	**C**	**H**	
C	0.0	1.0	0.2	2.9	14.9	19.0
Cu	0.0	0.9	0.0	0.0	0.3	1.2
H	0.3	9.4	1.3	11.2	41.6	63.8
N	0.0	0.0	0.0	0.2	1.7	1.9
O	0.8	1.3	0.0	0.9	11.0	14.0
d_e total (%)	1.1	12.6	1.5	15.2	69.5	

Table S3 Percentage contribution of elements to the internal and external surface of $\{[Cu(II)(L_4H_2)_2].2MeOH\}_n$ (**2**) using Hirschfeld surface analysis (d_{norm}). *Note:* d_i = internal distance (from the nucleus to the surface), d_e = external distance (between surface and nucleus of nearest neighbour) in Å.

d_i	**d_e**					**d_i total (%)**
	Cu	**O**	**N**	**C**	**H**	
C	0.2	1.3	0.4	3.0	13.3	18.2
Cu	0.0	0.0	0.5	0.2	0.5	1.2
H	0.5	10.7	0.6	8.1	46.4	66.3
N	0.5	0.1	0.0	0.4	0.9	1.9
O	0.0	0.0	0.1	1.2	11.1	12.4
d_e total (%)	1.2	12.1	1.6	12.9	72.2	

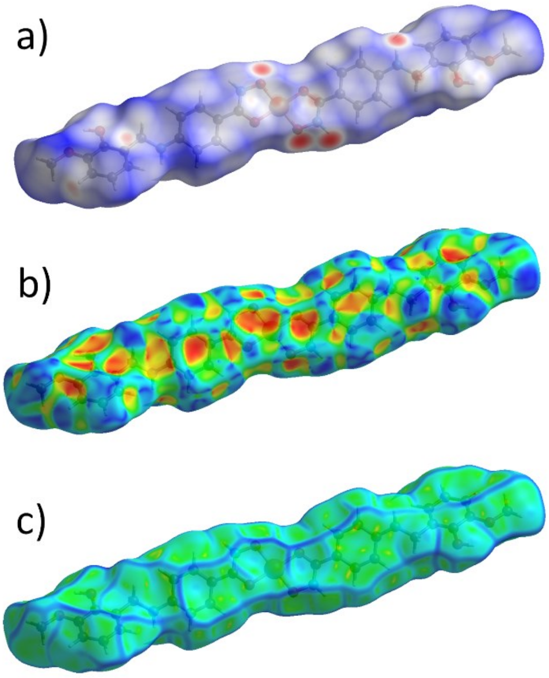

Figure S4 Hirschfeld surface analysis outputs for $[Cu(II)(L_3H_2)_2]_n$ (**1**) using the d_{norm} (a), shape index (b) and curvedness (c) function.

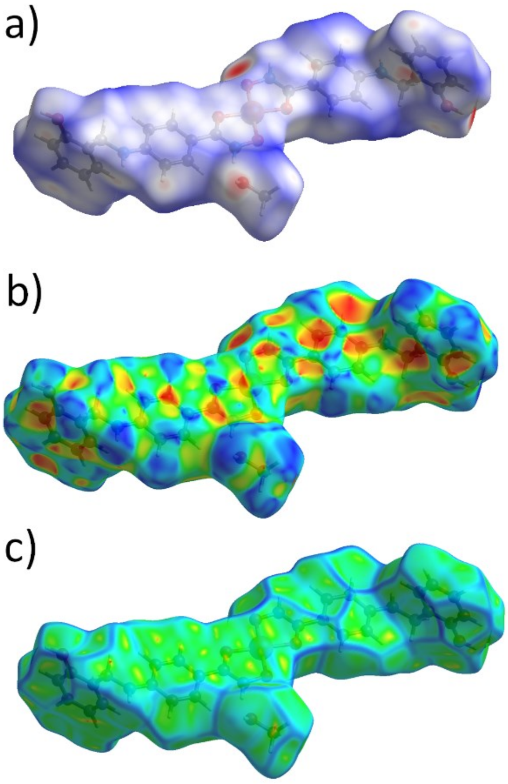

Figure S5 Hirschfeld surface analysis outputs for $\{[Cu(II)(L_4H_2)_2].2MeOH\}_n$ (**2**) using the d_{norm} (a), shape index (b) and curvedness (c) function.

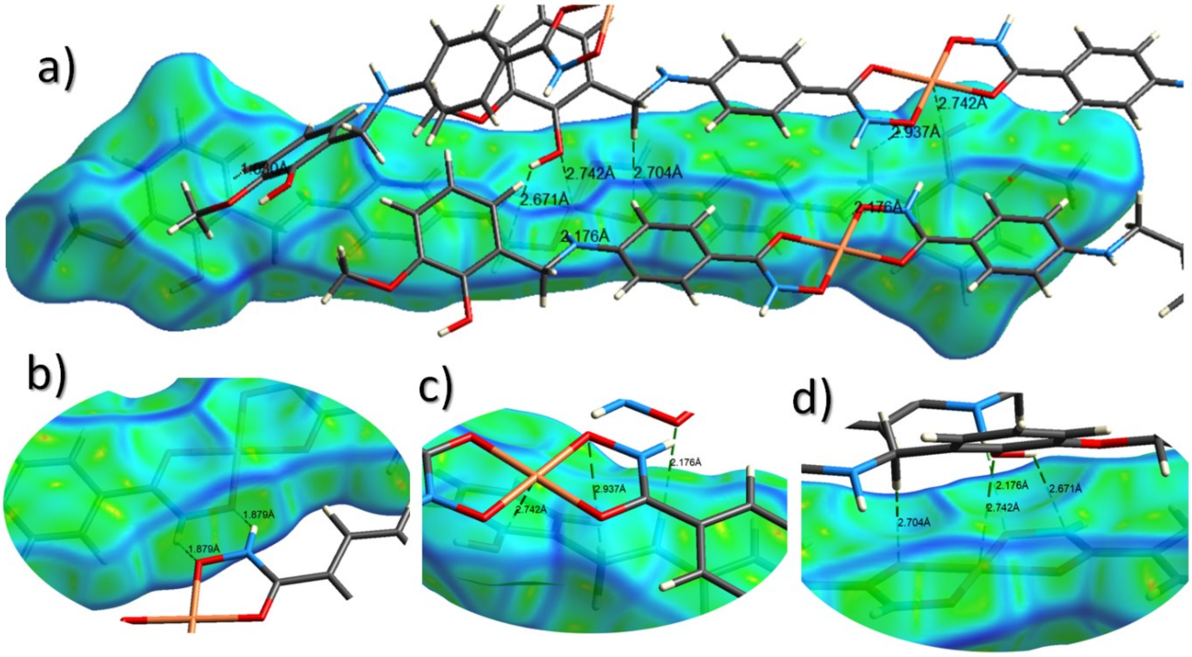

Figure S6 Hirshfeld surface analysis of $[Cu(II)(L_3H_2)_2]_n$ (**1**) using the curvedness function. Each figure corresponds to their d_{norm} equivalents shown in Figure 6 (main text). The green and blue colourations represent flat and significantly curved regions, respectively.

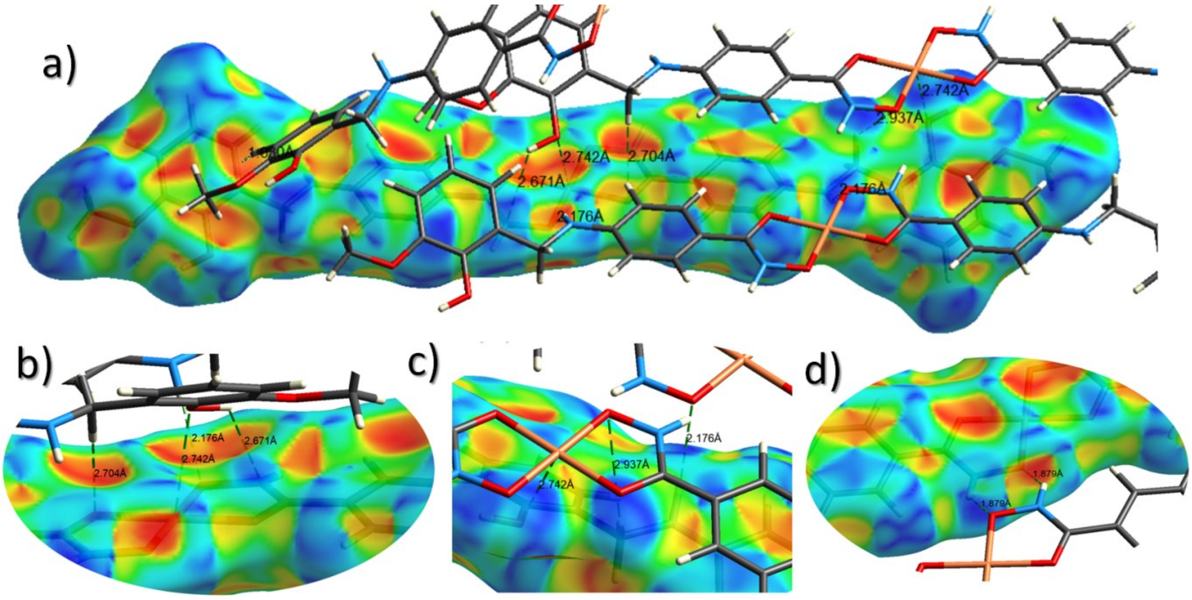

Figure S7 Hirshfeld surface analysis of $[Cu(II)(L_3H_2)_2]_n$ (**1**) using the shape index function. Each figure corresponds to their d_{norm} and curvedness equivalents shown in Figures 6 (main text) and S6 (above). The blue and red regions represent convex (bump) and concave (hollow) surfaces, respectively and therefore when coupled indicates the presence of a significant interactions. A green region represents minimal contributions / interactions.

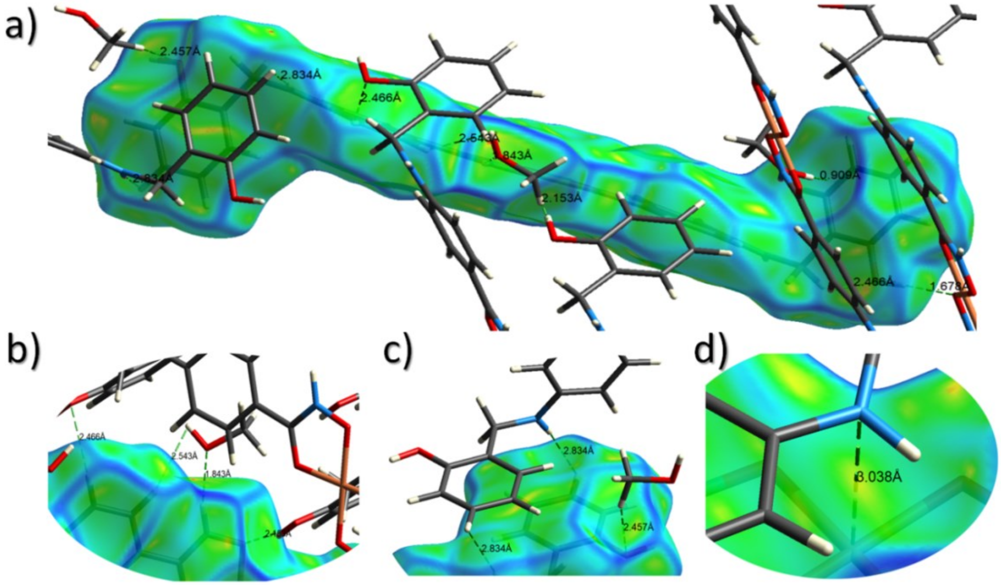

Figure S8 Hirshfeld surface analysis of {[Cu(II)(L_4H_2)$_2$].2MeOH}$_n$ (**2**) using the curvedness function. Each figure corresponds to their d_{norm} and curvedness equivalents shown in Figure 8 (main text). The green and blue colourations represent flat and significantly curved regions, respectively.

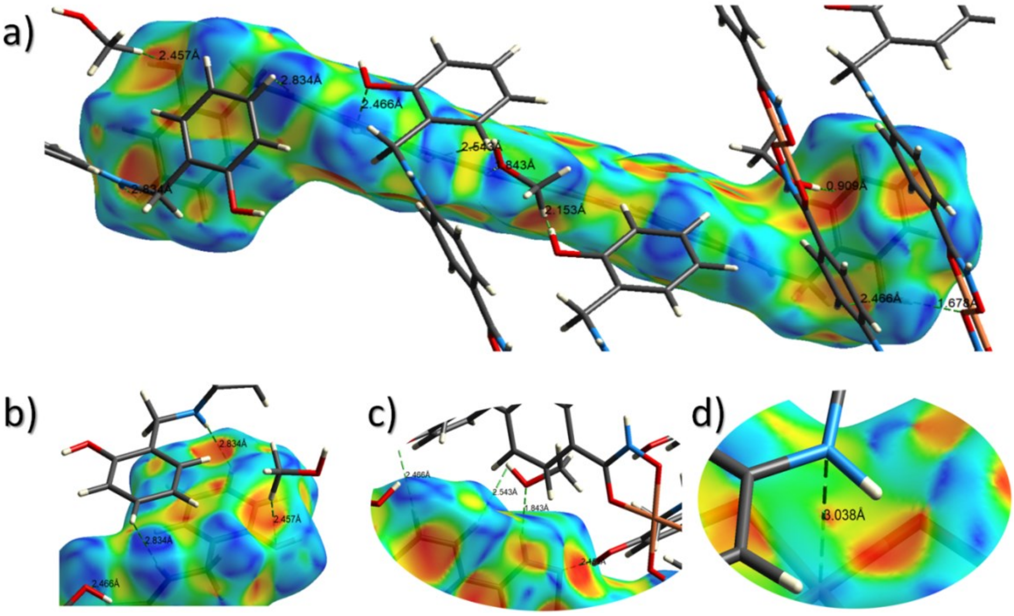

Figure S9 Hirshfeld surface analysis of {[Cu(II)(L_4H_2)$_2$].2MeOH}$_n$ (**2**) using the shape index function. Each figure corresponds to their d_{norm} and curvedness equivalents shown in Figures 8 (main text) and S8 (above). The blue and red regions represent convex (bump) and concave (hollow) surfaces, respectively and therefore when coupled indicates the presence of a significant interactions. Figure d further supports the presence of an interaction between Cu1 and N2′, highlighted by the concave red region of the Hirshfeld surface.

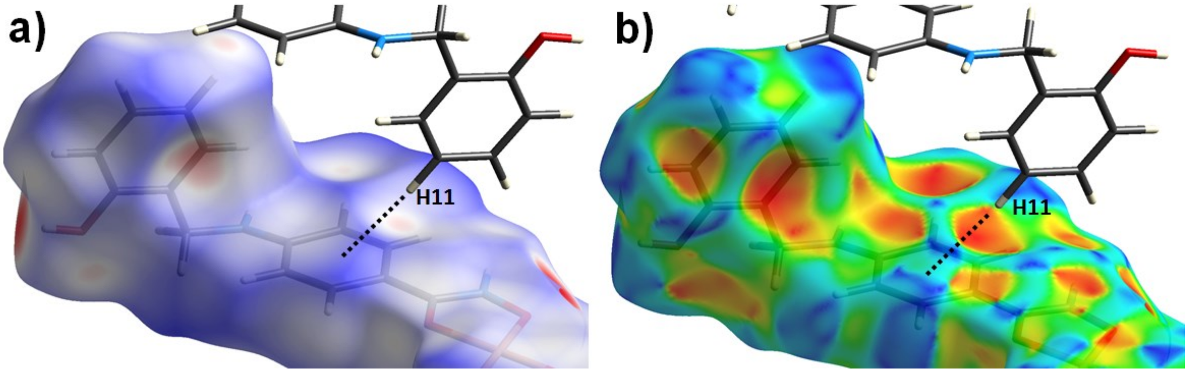

Figure S10 The d_{norm} (a) and shape index (b) Hirshfeld surfaces for **2**, highlighting the inter-chain C-H…π interaction: C11(H11)···[C2′-C7′]$_{centroid}$ = 3.44 Å (these are distances taken from the crystal structure data).

Table S4 Geometry optimisation studies on complexes **1** and **2**. The observed ligand conformations (observed in crystal structures) are given in green. Key: **bfm2d-180X** = $[Cu(II)(L_3H_2)_2]_n$ (**1**) (with an ~180° planar ligand orientation); **bfm2d-90X** = $[Cu(II)(L_3H_2)_2]_n$ (**1**) (with an ~90° planar ligand orientation); **bfm3d-180X** = $[Cu(II)(L_4H_2)_2]_n$ (**2**) (with an ~180° planar ligand orientation and **bfm3d-90X** = $[Cu(II)(L_4H_2)_2]_n$ (**2**) (with an ~90° planar ligand orientation).

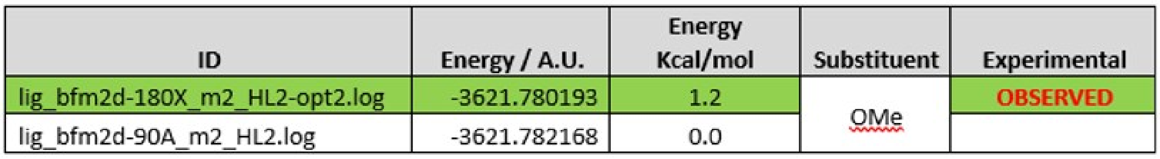

ID	Energy / A.U.	Energy Kcal/mol	Substituent	Experimental
🟩 lig_bfm2d-180X_m2_HL2-opt2.log	-3621.780193	1.2	OMe	OBSERVED
lig_bfm2d-90A_m2_HL2.log	-3621.782168	0.0		

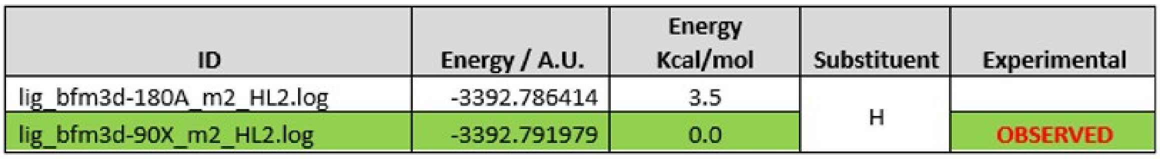

ID	Energy / A.U.	Energy Kcal/mol	Substituent	Experimental
lig_bfm3d-180A_m2_HL2.log	-3392.786414	3.5	H	
🟩 lig_bfm3d-90X_m2_HL2.log	-3392.791979	0.0		OBSERVED

References

1. C. F. Macrae, I. J. Bruno, J. A. Chisholm, P. R. Edgington, P. McCabe, E. Pidcock, L. Rodriguez-Monge, R. Taylor, J. van de Streek, P. A. Wood, New Features for the Visualization and Investigation of Crystal Structures. *J. Appl. Cryst.,* 41 (2008) 466-470.